STRENGTHENING OF TWO-WAY R.C SLABS USING LOWER CONCRETE LAYER REINFORCED BY FRP BARS

.

ABSTRACT

Aims: Study the strengthening of two-way reinforced concrete slabs using lower concrete layer reinforced by FRP bars.

Study design: Parametric study is carried out by varying the material type, thickness of strengthening layer, spacing between strengthening layer reinforcement bars, cross sectional area of this reinforcement and the type of the strengthening reinforcement.

Methodology: This study presents the efficiency of adding lower concrete layer reinforced by different materials to increase the flexural strength for two-way R.C slabs. Eleven half-scale two-way R.C slab specimens were prepared and tested under four point bending. One of these slabs was unstrengthened and considered as a control specimen. The other specimens were strengthened by using different lower concrete layers reinforced mainly by fiber reinforced polymer (FRP) bars. The parameters of this study included the material type (reinforcement steel, glass fiber and carbon fiber), the thickness of strengthening layer (30 & 50 mm), spacing between strengthening layer reinforcement bars (100 & 200 mm), cross sectional area of this reinforcement (A & 2A) and the type of the strengthening reinforcement (FRP bars & FRP strips).

Results: The experimental results included cracking load, ultimate load, load-deflection relationships, relative ductility, and flexural stiffness.

Conclusion: The experimental results showed an improvement in the flexural behavior of the strengthened specimens compared to control specimen. The flexural strength of the different strengthened specimens increased by 37% to 112% compared to the control specimen. Moreover, a finite element models were developed by ANSYS (version 15) to simulate all the tested specimens. The results calculated based on FEM models were in good agreement with the corresponding experimental ones. However, the calculated ultimate loads were slightly higher than the experimental ultimate loads up to 12%.

Keywords: Two-way R.C slabs, Flexure Failure, strengthening, Fiber Reinforced Polymer and finite element analysis.

1. INTRODUCTION

Strengthening and repair of reinforced concrete structures is frequently required due to inadequate maintenance, excessive loading, change in use or in code of practice and exposure to adverse environmental condition [1]. Several strengthening techniques have

25 been developed by different traditional techniques including steel plate bonding, external
26 prestressing and reinforced concrete jacting [2,3,4,5]. Reinforced concrete solid slabs are
27 used in floors and as decks of bridges. Slabs may span in one direction or in two directions
28 depending on the slab dimension and the surrounding supporting elements. Different
29 strengthening techniques have been developed so that its serviceability and strength can be
30 restored. Also, the strengthening of the structure should be done taking into consideration
31 the durability aspect. Nowadays, various strengthening techniques are available. However,
32 the selection of the proper technique depends on many factors; such as the deficiency
33 aspect of RC slabs, the cost of the proposed technique, the conditions to which the RC slabs
34 are exposed and the availability of the selected technique [1]. Recently, using FRP materials
35 to strengthen the different RC elements are gaining popularity due to their superior
36 properties which may exceed the steel. The FRP elements have high strength to weight
37 ratio, ease of application, non-magnetic and non-corrosive. Different FRP systems can be
38 applied to strengthen the RC slabs, these systems include externally bonded FRP strips,
39 near surface mounted elements and external post tension tendon [6,7,8,9,10]. This study
40 concerns with evaluate the using of RC lower layer reinforced by FRP bars as a
41 strengthening system for two-way RC slabs.
42
43
44 **2. EXPERIMENTAL INVESTIGATION**
45
46 Eleven specimens were cast and tested to investigate strengthening of two-way R.C slabs
47 using lower concrete layer reinforced by FRP bars. The tested specimens in this study were
48 half-scale models of a typical prototype solid slab structure with equal spans of 180 cm in
49 both directions. All the tested specimens were two-way simply supported slabs.
50
51
52 **2.1 Details of test specimens**
53
54 All the R.C specimens have square shape of 2000×2000 mm in plan. The thickness of the
55 control specimen and the rest of specimens prior to strengthening is 70 mm. The tested
56 specimens were designed to be simply supported along the four edges using line support on
57 each side. Normal mild steel bars of 8 mm diameters with 200 mm spacing in each direction
58 were used as main reinforcement. Full details of the control specimen and the other
59 specimen perior to strengthening, are shown in Fig. 1. The specimens are divided into six
60 groups and reference group, as shown in Table 1.
61
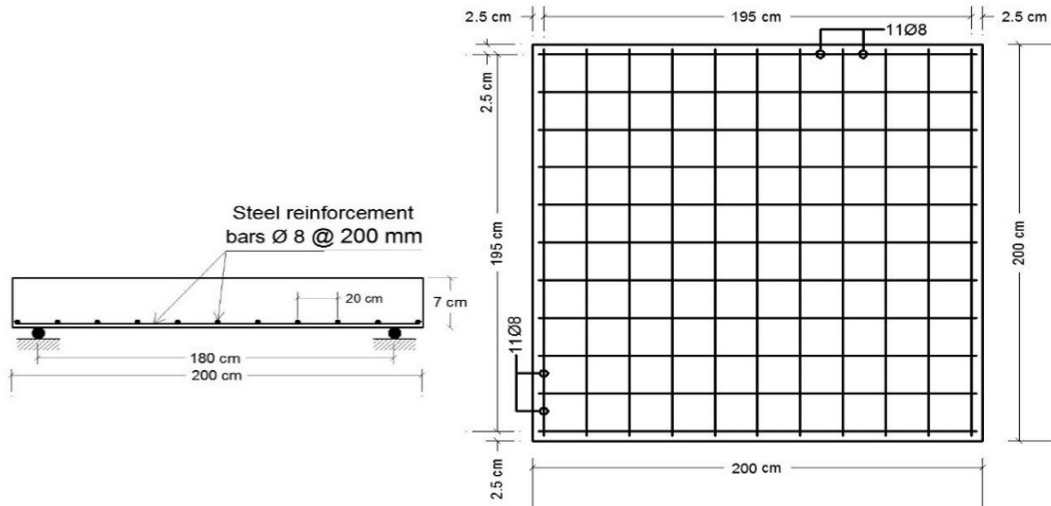
Fig. 1. Dimensions and reinforcement details of the control specimen and the other specimens prior to strengthening.

Table 1. The experimental test program.

Group	Specimen code	Specimen status	Strengthening layer			
			Reinforcement	Layer thickness (mm)	Bars/sheet spacing (mm)	**Area of reinforcement bars/sheets (mm^2)
Reference	C	control	---	---	---	---
First group	S-3-20-As		Steel bars	30	200	50.3
Second group	C-3-10-Ac/2		CFRP bars	30	100	28.3
	C-3-20-Ac				200	50.3
Third group	G-3-10-Ag/2		GFRP bars	30	100	28.3
	G-3-20-Ag	Strengthening			200	50.3
Fourth group	G-5-10-Ag/2		GFRP bars	50	100	28.3
	G-5-20-Ag				200	50.3
Fifth group	G-3-10-Ag		GFRP bars	30	100	50.3
	G-5-10-Ag			50	100	50.3
Sixth group	GS-1.5-20-Ag		GFRP sheets*	15	200	70.0

* Externally bonded

** The area of steel or FRP cross-sectional

2.2 Preparation of test specimens

The moulds were prepared and assembled in order to fulfill the required dimensions of the specimens. After the steel reinforcement were installed, concrete mix was placed then the concrete was vibrated mechanically and the concrete surface was finished. After curing

76   period the specimens were left in the lab atmosphere until strengthening date. Ten
77   specimens were strengthened, nine specimens strengthened by FRP element and one
78   specimen by steel bars. Two strengthening techniques were used. For first technique;
79   specimen surface was notched to achieve rough surface using an angle grinder. 10 mm
80   diameter holes were drilled at the arranged positions of anchors (each 400 mm in both
81   directions with staggered shape). Anchors were fixed using sikadur 31 CF and the
82   reinforcement bars were installed to the specimen. Surface of specimens was sprinkled by
83   Addibond 65 to improve the bond between original specimen and strengthening layer, then
84   concrete layer was placed and finished. For second technique; Specimen surface removed
85   from any unevenness and Sikadur 330 epoxy resin was applied at the areas where GFRP
86   strips were installed in the two directions by using special roller. Figs. (2, 3 & 4) illustrates
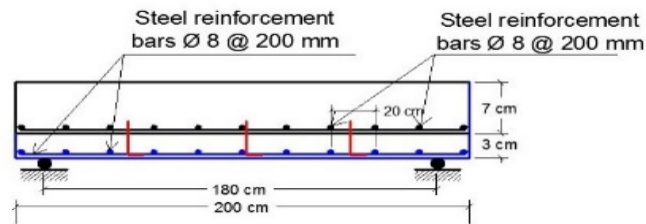87   details of strengthening systems.
88
89

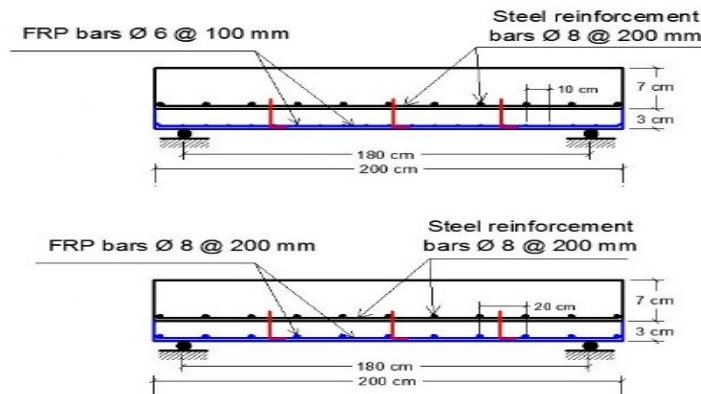**Fig. 2. Adding lower concrete layer reinforced by steel reinforcement mesh**

90

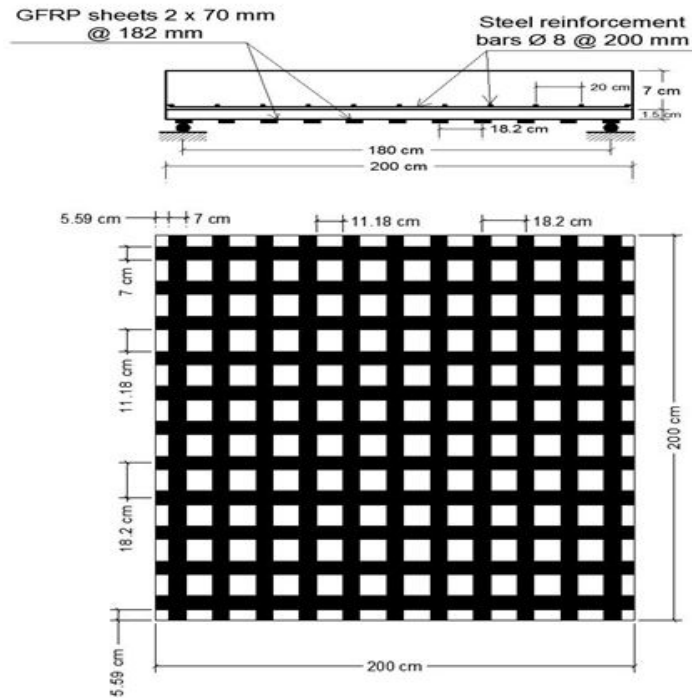**Fig. 3. Adding lower concrete layer reinforced by FRP bars**

91

Fig. 4. Adding lower concrete layer reinforced externally by bonded GFRP strips

92
93 **3. MATERIAL PROPERTIES.**

94
95 **3.1 Concrete**

96
97 Suitable mix of 305 kg/cm2 cubic compressive strength after 28 days was used. The
98 constituents of concrete mix and its proportions are presented in Table 2.

99
100 **Table 2. The constituents of concrete mix.**
101

Cement (Kg/m^3)	Crushed dolomite (Kg/m^3)	Sand (Kg/m^3)	Water (Liter/m^3)
350	1260	630	175

102
103 **3.2 FRP**

104
105 CFRP and GFRP bars were locally fabricated using pultrusion process with polyester
106 polymer, then their surfaces were coated by sand layer to improve its bond. The Mechanical
107 properties of FRP bars are given in Table 3. GFRP sheets are, also, locally fabricated. The
108 number of strands in the GFRP strips is the same as in the GFRP bars. The Mechanical
109 properties of GFRP sheets are given in Table 4.

110
111

112 **3.3 steel bars**
113
114 8 mm diameter of normal mild steel bars are used to reinforce the tested specimens and,
115 also, were used as reinforcement for strengthening layer for specimen (S-3-20-As).
116

117 **Table 3. Dimensional and mechanical properties of FRP bars**

Property	GFRP bars		CFRP bars	
Diameter of bars	8 mm	6 mm	8 mm	6 mm
Area of bars	50 mm^2	28.3 mm^2	50 mm^2	28.3 mm^2
Area of fibers	14.55 mm^2	7.75 mm^2	12.8 mm^2	6.4 mm^2
Fiber ratio by area	30%	28%	26%	23%
Tensile strength of fibers	13700 kg/cm^2		14000 kg/cm^2	
Modulas of elasticity of fibers	900000 kg/cm^2		2100000 kg/cm^2	
Strain at failure	15000 x 10^{-6}		6600 x 10^{-6}	

118
119 **Table 4. Dimensional and mechanical properties of FRP sheets**

Property	GFRP
Fabric design thickness	1 mm
Fabric width	7 cm
Tensile strength	22500 kg/cm^2
Modulus of elasticity	760000 kg/cm^2
Strain at failure	2.80%

120
121
122 **4. TEST PROCEDURE**
123
124 The loading system consisted of rigid system of reaction frame, 100 ton capacity, and
125 hydraulic jack, 100 ton capacity, connected to electrical pump. The specimens were tested
126 under vertical concentrated load which is distributed to four equal point concentrated loads
127 acting on the slab upper surface by means of rigid steel frame, as shown in Fig. 5. The
128 specimens were simply supported on line supports at the four sides over a clear span of
129 1800 mm. Vertical deflection, first cracking load and ultimate failure load, were recorded.
130 Five linear variable differential transducers (LVDTs) mounted at the bottom soffit of the
131 specimen for measuring deflections at bottom face (tension side), as shown in Fig. 6. Cracks
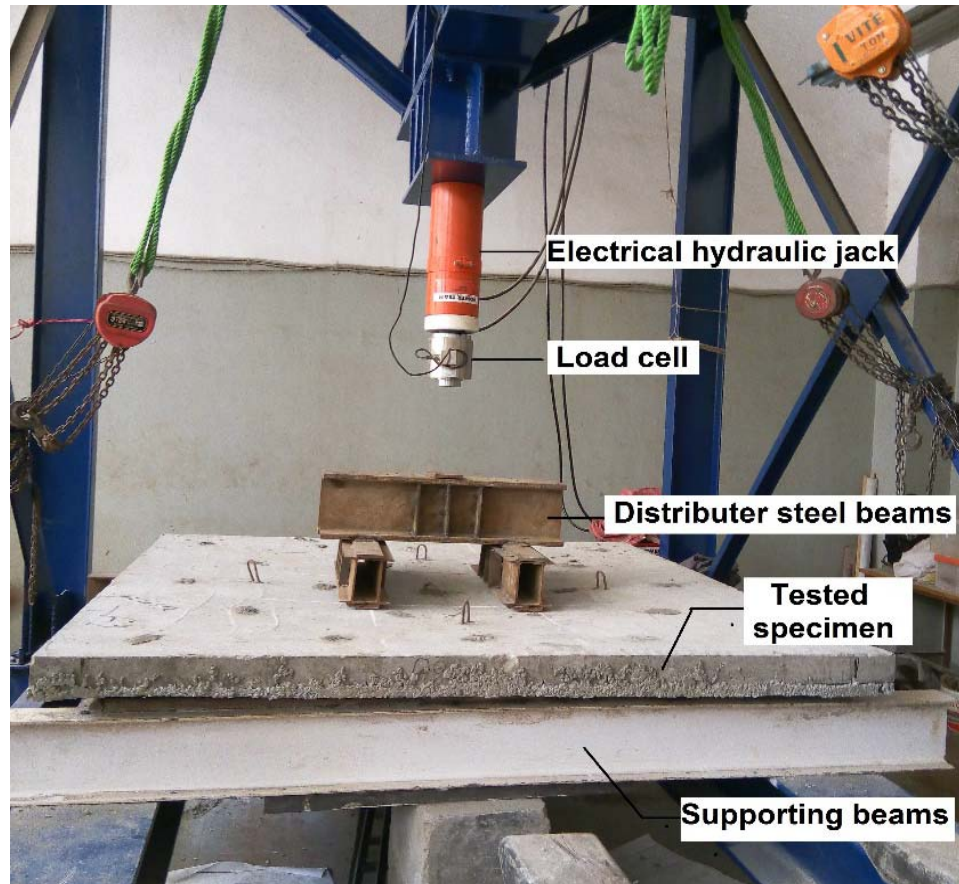132 propagation was monitored after each load increment up to failure.
133
134
135
136
137

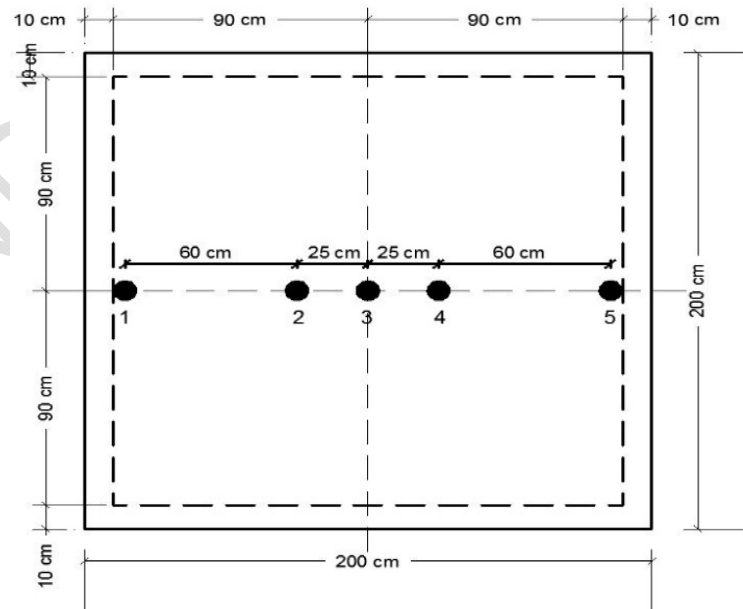**Fig. 5. Test set up**

Fig. 6. LVDT locations (bottom side).

5. RESULTS AND DISCUSSION

For the all tested specimens, the relationship between the central deflection at mid-point (point 3) and the applied load was plotted and the crack propagation was monitored with load increasing till failure, Also, the cracking load and ultimate load were recorded. Comparisons between the results of different specimens were carried out to reveal the effect of the parameters considered in this study.

5.1 Load-deflection relationships

All the strengthening systems used in this study led to a significant increase in the strength and the rigidity of the strengthened specimens in comparison with the control specimen. At the same loading level, lower deflection values were recorded for strengthened specimens, either with steel reinforcement, GFRP or CFRP bars, in comparison with the control specimen, as shown in Figs. (7 to 16).

5.1.1 Effect of strengthening layer thickness

The used layers thickness are 30 & 50 mm, respectively. The effect of this parameter could be observed by studying the behavior of specimens G-3-10-Ag/2 & G-5-10-Ag/2, specimens G-3-20-Ag & G-5-20-Ag and specimens G-3-10-Ag & G-5-10-Ag, as shown in Figs. (7, 8 & 9).
As expected, adding the strengthening layer led to improve the flexural behavior. The ultimate load was higher than that of control specimen by 76% and 112% for strengthening layer with thickness 30 mm and 50 mm, respectively. Also, the deflection was reduced by 83.8% and 97.5%, respectively at ultimate recorded load of control specimen.
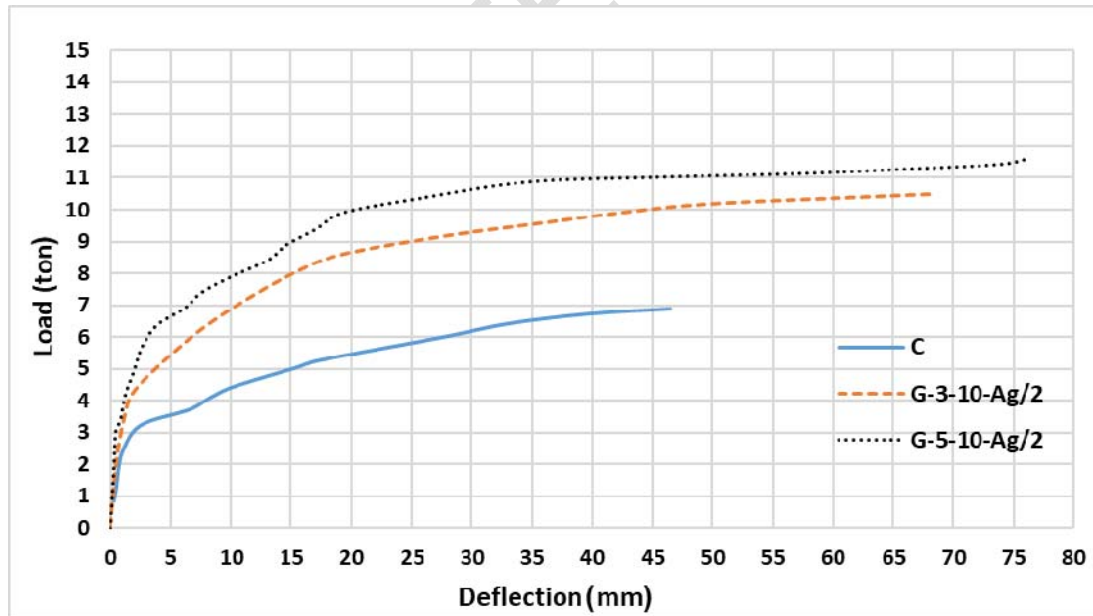

Fig. 7. Comparison between Load-Central deflection relationships of the specimens (G-3-10-Ag/2), (G-5-10-Ag/2), and (C).
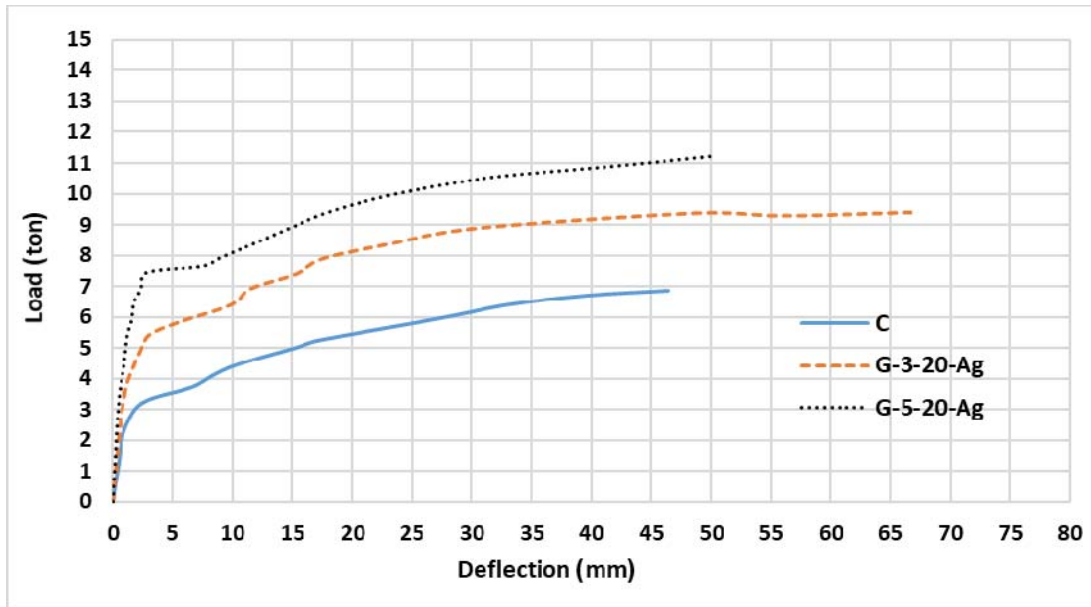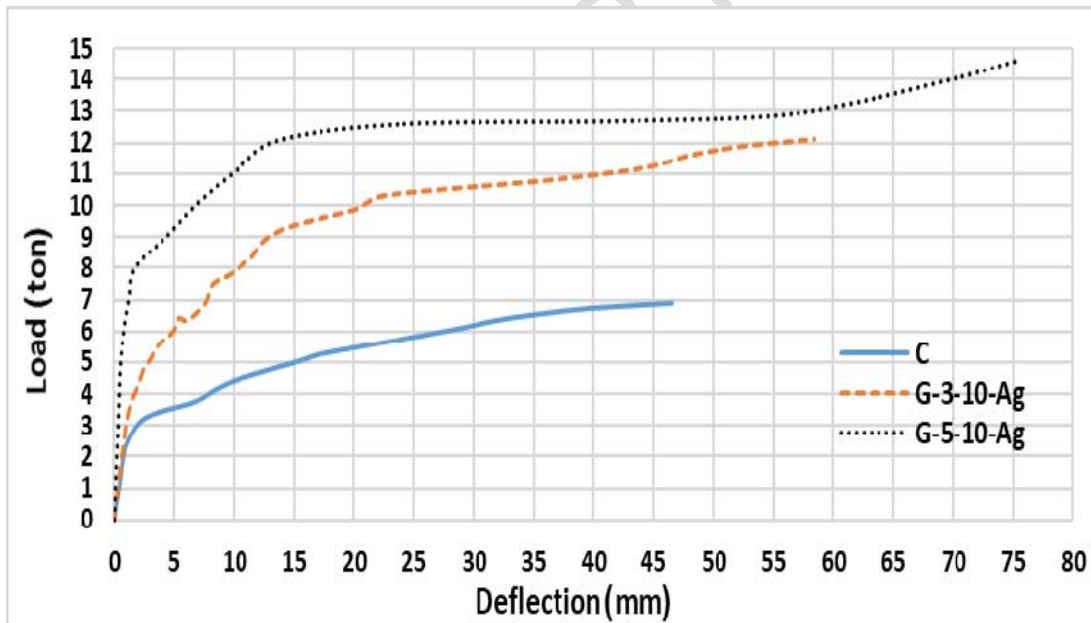
198
199
200 **Fig. 8. Comparison between Load-Central deflection relationships of the specimens**
201 **(G-3-20-Ag), (G-5-20-Ag), and (C).**
202

203
204
205 **Fig. 9. Comparison between Load-Central deflection relationships of the specimens**
206 **(G-3-10-Ag), (G-5-10-Ag), and (C).**
207
208
209
210
211

212 **5.1.2 Effect of strengthening material type**
213

214 The effect of this parameter could be observed by studying the behavior of specimens S-3-
215 20-As, C-3-20-Ac & G-3-20-Ag, as shown in Fig. 10, which correspond to three types of
216 strengthening materials: steel reinforcement bars, CFRP bars, and GFRP bars.
217 All the materials used in strengthening led to improve the flexural behavior, where the
218 ultimate load was increased and the deflection at the same loading values was decreased.
219 CFPR bars was the best material, the ultimate load was increased by 68%. However, GFRP
220 bars and steel bars have close ultimate load of 137 % and 138%, respectively of the
221 corresponding control specimen value. The deflections at ultimate load of control specimen
222 was reduced by 80.6%, 75.3% and 92% for specimens strengthened by CFRP, GFRP and
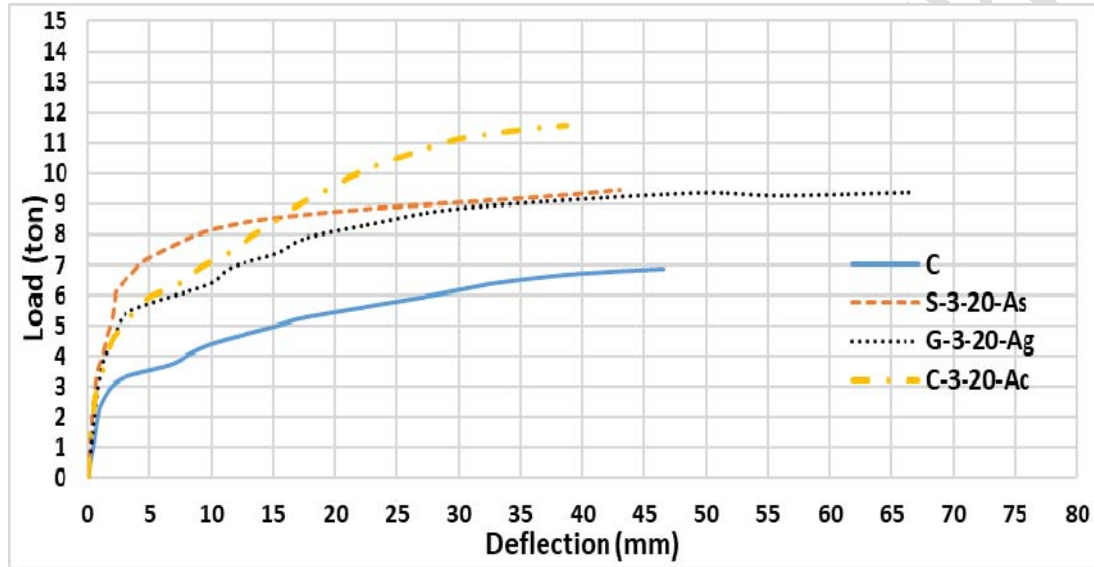223 steel bars, respectively.
224

225
226
227 **Fig. 10. Comparison between Load-Central deflection relationships of the specimens**
228 **(S-3-20-As), (C-3-20-Ac), (G-3-20-Ag), and (C).**
229
230 **5.1.3 Effect of spacing between reinforcement bars**
231

232 The effect of this parameter could be observed by studying the behavior of three specimen
233 groups (G-3-10-Ag/2 & G-3-20-Ag, G-5-10-Ag/2 & G-5-20-Ag and C-3-10-Ac/2 & C-3-20-Ac),
234 as shown in Figs. (11, 12 & 13). The used spacing are 100 & 200 mm, respectively.
235 Reducing the spacing between bars with keeping the same cross-sectional area led to
236 increase the ultimate load by 53%, 69% and 95% for the three studied groups, respectively
237 compared to that recorded for the control specimen.
238 The effect of this parameter was more pronounced for CFRP, not only on the ultimate load
239 but also on the deflection reduction, which decreased at maximum recorded load of control
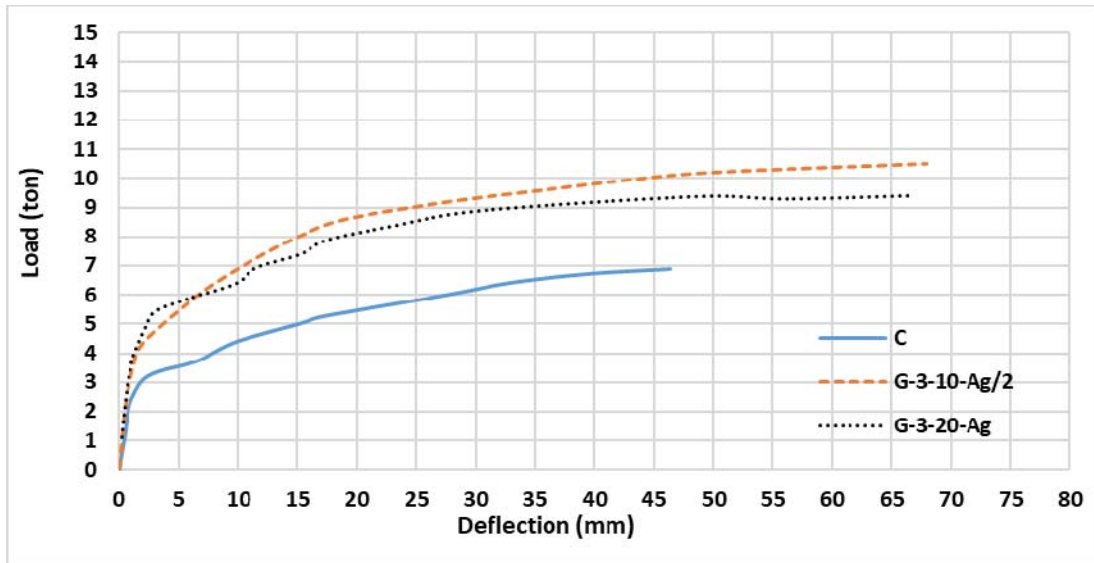240 specimen by 93.1% when the spacing was reduced from 200 mm to 100 mm.

241
242
243
244
245
246
247

248
249
250 **Fig. 11. Comparison between Load-Central deflection relationships of the specimens**
251 **(G-3-10-Ag/2), (G-3-20-Ag), and (C).**
252

253
254
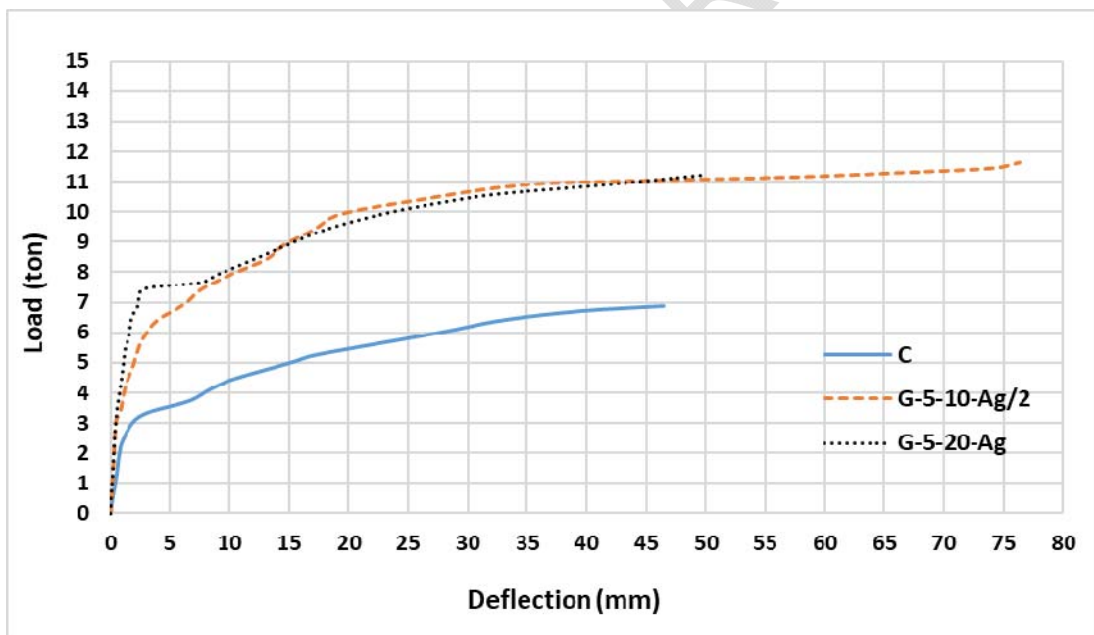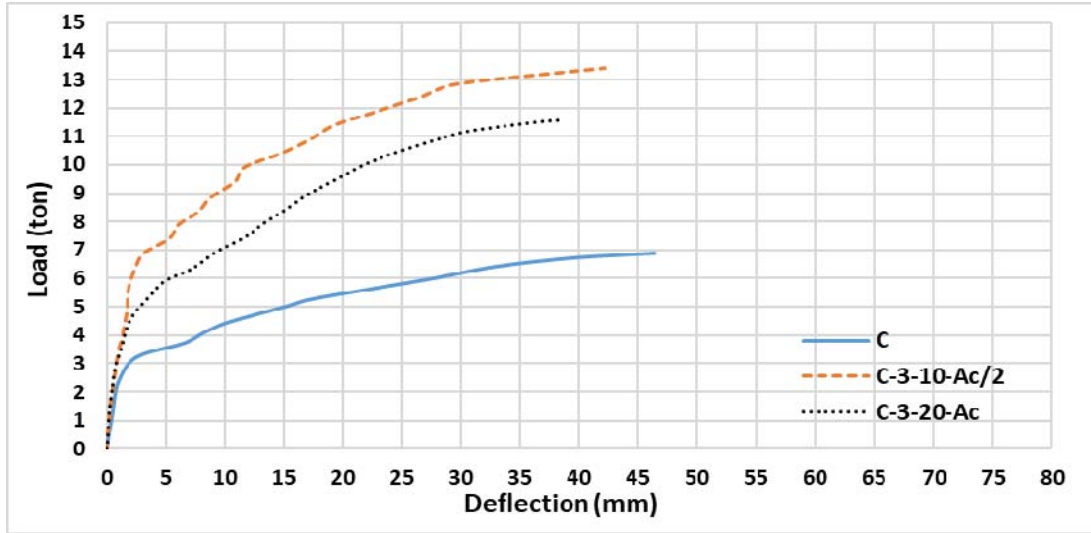255 **Fig. 12. Comparison between Load-Central deflection relationships of the specimens**
256 **(G-5-10-Ag/2), (G-5-20-Ag), and (C).**
257

258
259
Fig. 13. Comparison between Load-Central deflection relationships of the specimens (C-3-10-Ac/2), (C-3-20-Ac) and (C).

262
5.1.4 Effect of x-sectional area of reinforcement bars

264
The effect of this parameter could be observed by studying the behavior of specimens (G-3-10-Ag/2 & G-3-10-Ag and specimens G-5-10-Ag/2 & G-5-10-Ag), as shown in Figs. (14 & 15). For the used areas A & 2A mm, respectively.
As expected, doubling the x-sectional area of bars led to increase the ultimate load by 76% and 112% for specimens strengthening by adding RC layer reinforced by GFRP bars with thickness 30 mm and 50 mm, respectively, also, the deflection at maximum recorded load of control specimen was reduced by 83.8% and 97.5%, respectively in compared with control specimen.

273
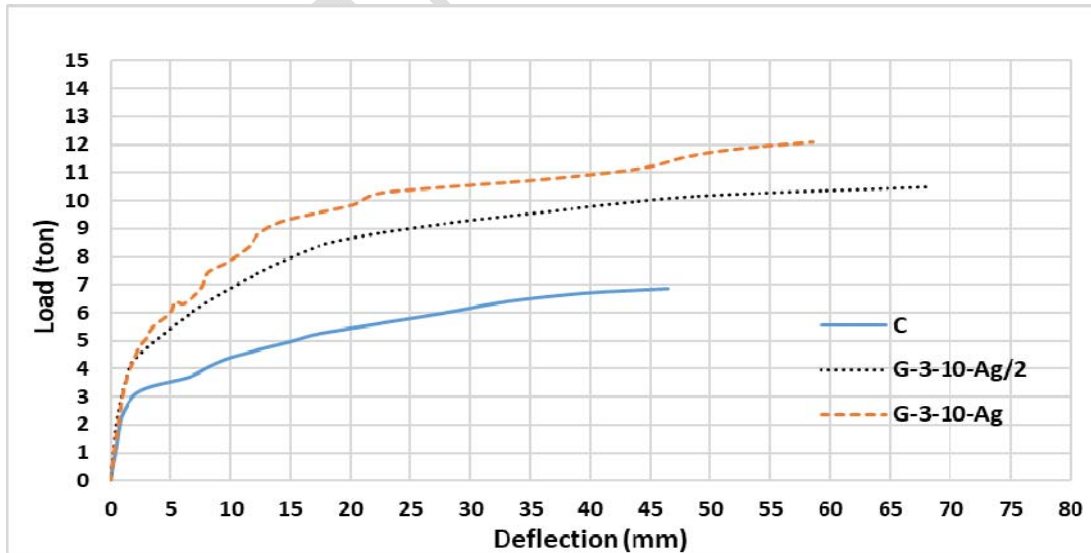
274
275
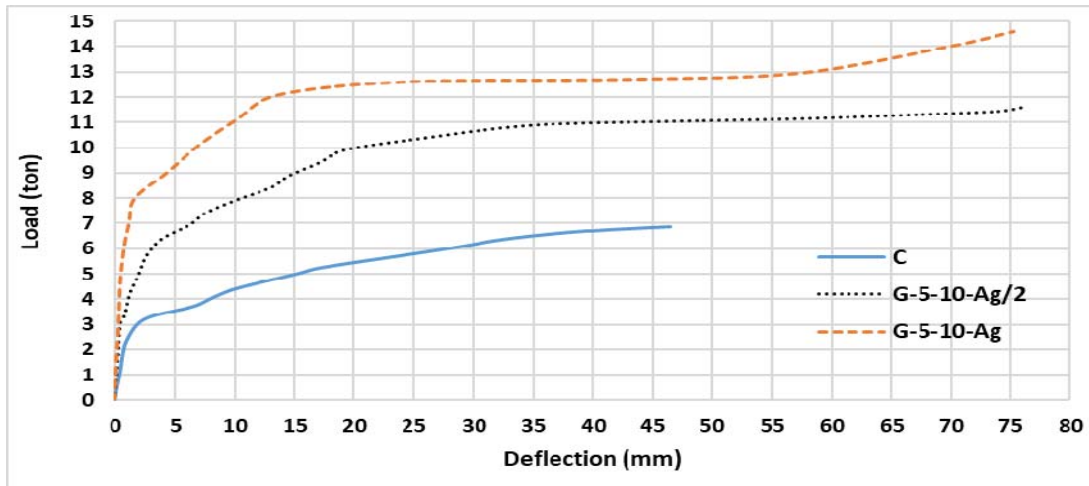**Fig. 14. Comparison between Load-Central deflection relationships of the specimens (G-3-10-Ag/2), (G-3-10-Ag), and (C).**

278
279
280 **Fig. 15. Comparison between Load-Central deflection relationships of the (G-5-10-**
281 **Ag/2), (G-5-10-Ag), and (C).**
282

283 **5.1.5 Effect of strengthening method**

284 The effect of this parameter could be observed by studying the behavior of specimens (G-3-
285 20-Ag & GS-1.5-20-Ag), as shown in Fig. 16, which correspond to two types of strengthening
286 methods. The first type was adding 30 mm lower concrete layer reinforced by GFRP bars
287 mesh, and the second was adding 15 mm lower concrete layer reinforced by externally
288 bonded GFRP sheets.
289 The two strengthening techniques led to increase the ultimate load by 53% and 71% for the
290 first and second technique, respectively compared to the control specimen, also, the
291 deflection at maximum recorded load of control specimen was reduced by 75.3% and
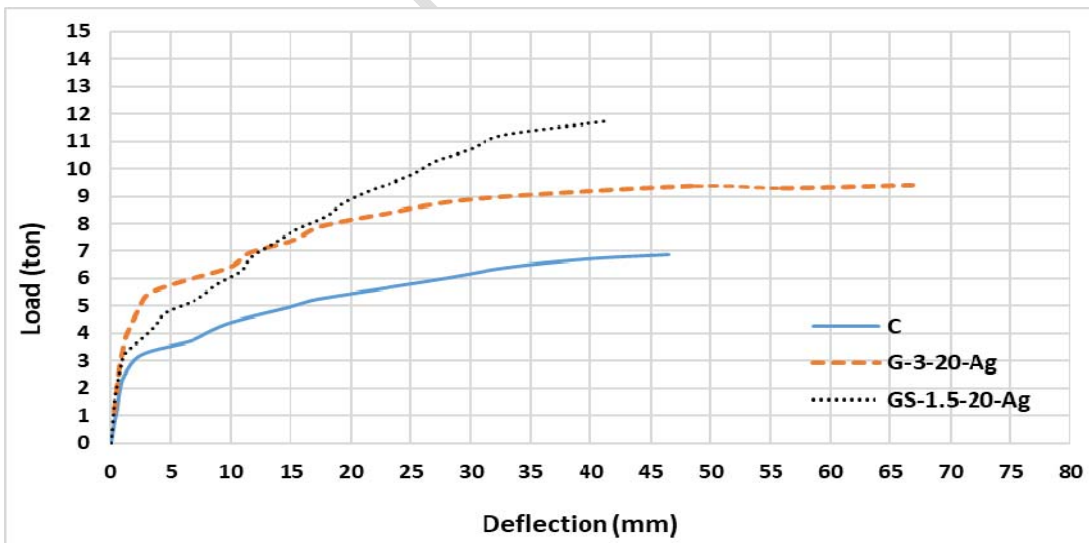292 75.9%, respectively in compared with control specimen.
293

294
295
296 **Fig. 16. Comparison between Load-Central deflection relationships of the (G-3-20-Ag),**
297 **(GS-1.5-20-Ag), and (C).**
298

5.2 Cracking load and ultimate load.

300

301 Table. 5 presents the deflection and load values at first cracking and at failure, and also the
302 ductility and the stiffness indices, for all the tested specimens. The specimen (G-5-10-Ag),
303 had the highest ultimate load, higher than that of control specimen by 112%. This was
304 expected because the former specimen has the more effective strengthening system with a
305 lower concrete layer of 50 mm thickness (the biggest thickness) reinforced by GFRP bars of
306 double cross sectional area. The specimen (C-3-10-Ac/2) had the highest ultimate load
307 value, compared to all the specimens of lower layer of 30 mm thickness, the ultimate load of
308 this specimen was higher than that of control specimen by 95%. The high tensile strength of
309 carbon fiber and the small spacing between the CFRP bars (high surface area) may explain
310 the efficient strengthening system of specimen (C-3-10-Ac/2). Fig. 17 shows cracking load
311 and ultimate load values for all specimens.

312

313 **Table. 5. Main results of the tested specimens.**

314

Specimen code	1st cracking		Ultimate		$\frac{P_{ult} \text{(specimen)}}{P_{ult} \text{(control)}}$	Ductility $\Delta_{ul} / \Delta_{cr}$	$K_i = P_{cr}/\Delta_{cr}$ (t/mm)	$K_u = \frac{P_{ul}-P_{cr}}{\Delta_{ul}-\Delta_{cr}}$ (t/mm)	Stiffness Degradation $\frac{(K_i-K_u) \times 100}{K_i}$
	Load (ton)	Δ_{cr} def. (mm)	Load (ton)	Δ_{ul} ult. (mm)					
C	2.00	0.79	6.88	46.50	1.00	58.86	2.53	0.11	95.79
S-3-20-As	4.00	1.23	9.46	43.10	1.38	34.92	3.24	0.13	95.98
C-3-10-Ac/2	5.00	1.75	13.40	42.17	1.95	24.06	2.85	0.21	92.71
C-3-20-Ac	4.00	1.50	11.58	38.78	1.68	25.85	2.67	0.20	92.38
G-3-10-Ag/2	4.50	2.50	10.50	68.00	1.53	27.20	1.80	0.09	94.91
G-3-20-Ag	4.00	1.18	9.40	66.90	1.37	56.79	3.40	0.08	97.58
G-5-10-Ag/2	5.10	2.00	11.64	76.35	1.69	38.17	2.55	0.09	96.55
G-5-20-Ag	4.00	0.74	11.23	50.00	1.63	67.27	5.38	0.15	97.27
G-3-10-Ag	3.00	0.98	12.10	58.46	1.76	59.55	3.06	0.16	94.82
G-5-10-Ag	8.00	1.67	14.59	75.25	2.12	45.09	4.79	0.09	98.13
GS-1.5-20-Ag	5.50	7.10	11.74	41.16	1.71	5.14	0.69	0.19	72.62

315
316
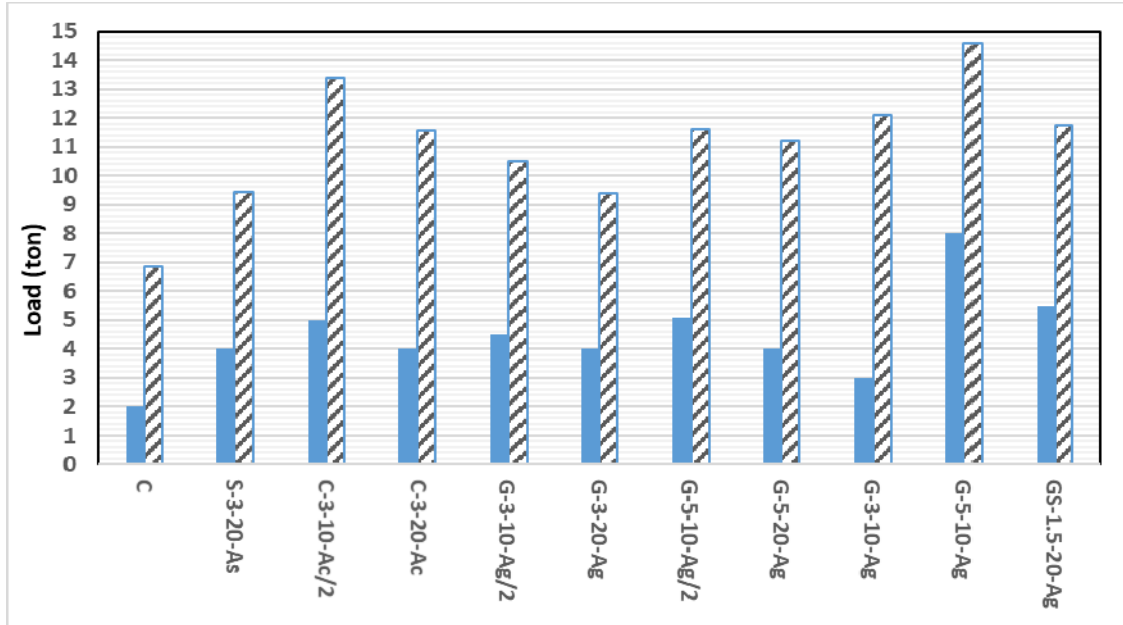
Fig. 17. Cracking and ultimate load for all specimens

5.3 Ductility

Ductility means the ability of a member to undergo inelastic deformations beyond the yield deformation without any considerable loss of load bearing capacity. The ductility of the specimens was considered as the ratio of the deflection at ultimate load to the deflection at first crack load as shown in Table. 5. Generally, specimens strengthened by adding lower concrete layer reinforced by GFRP bars are better than specimens strengthened by adding lower concrete layer reinforced by CFRP bars due to lower modulas of elasticity for GFRP than CFRP, but specimen strengthened by externally bonded GFRP sheets had the less ductility at all due to the high ability of sheets to debond.

5.4 Stiffness

The un-cracked stiffness Ki and the ultimate stiffness Ku were obtained from the load-deflection values of the tested specimens, as presented in Table. 5. It shows that the un-cracked stiffness (Ki) is almost, increased for the majority of the tested specimens. Adding lower concrete layer reinforced by reinforcement steel, CFRP& GFRP bars mesh led to increase Ki while adding lower concrete layer reinforced by externally bonded GFRP sheets led to decrease Ki.

5.5 Cracking behavior and mode of failure.

All the tested specimens were loaded until failed due to flexure. For all specimens, the first crack was recorded, cracks propagation were monitored, and the plane of failure was observed to investigate the cracking and failure behavior. Two modes of failure are expected, the first was flexure failure of the strengthening slab as a one units, while the second type is the debonding between the strengthening layer and the original slab. All specimens were failed by flexure failure with partial debonding between the strengthening

347 layer and the original slab. Table. 5. shows the load value corresponding to cracking
348 initiation (P_{cr}). Cracks began firstly at the slab tension side under the four point load forming
349 square lines. As the applied loads increase the number and width of the cracks increase
350 then new cracks develop and begin to propagate towards the slab edges in diagonal
351 directions towards the slab corners. The failure surface of the tested specimens was
352 carefully recorded. Strengthening systems led to an increase of the first crack load and, also,
353 its rates to the ultimate load of the tested specimens. A typical crack pattern is shown in Fig.
354 18 & 19 for control specimen and specimen G-3-10-Ag/2, respectively. For specimen GS-
355 1.5-20-Ag, where GFRP strips were externally bonded, it was failed due to debonding of the
356 strengthening strips, as shown in Fig. 20.
357
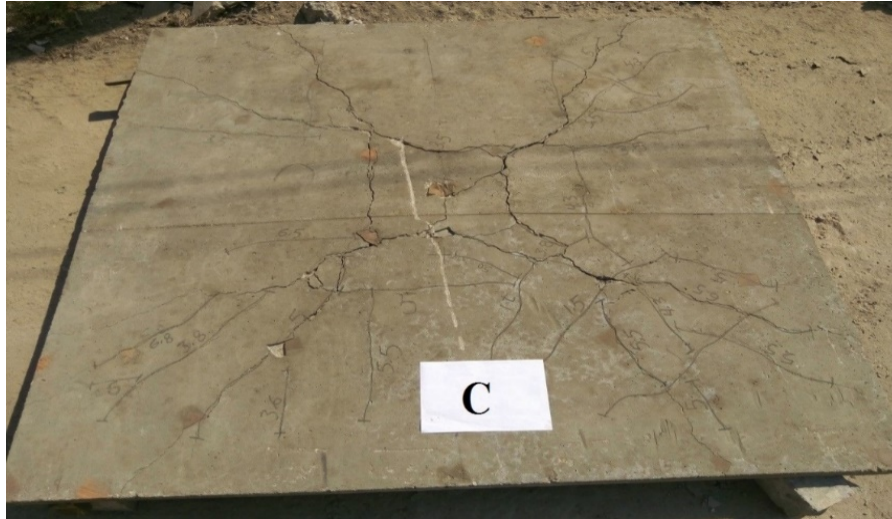
358
359
360 **Fig. 18. Cracking pattern of specimen (C).**
361

362
363
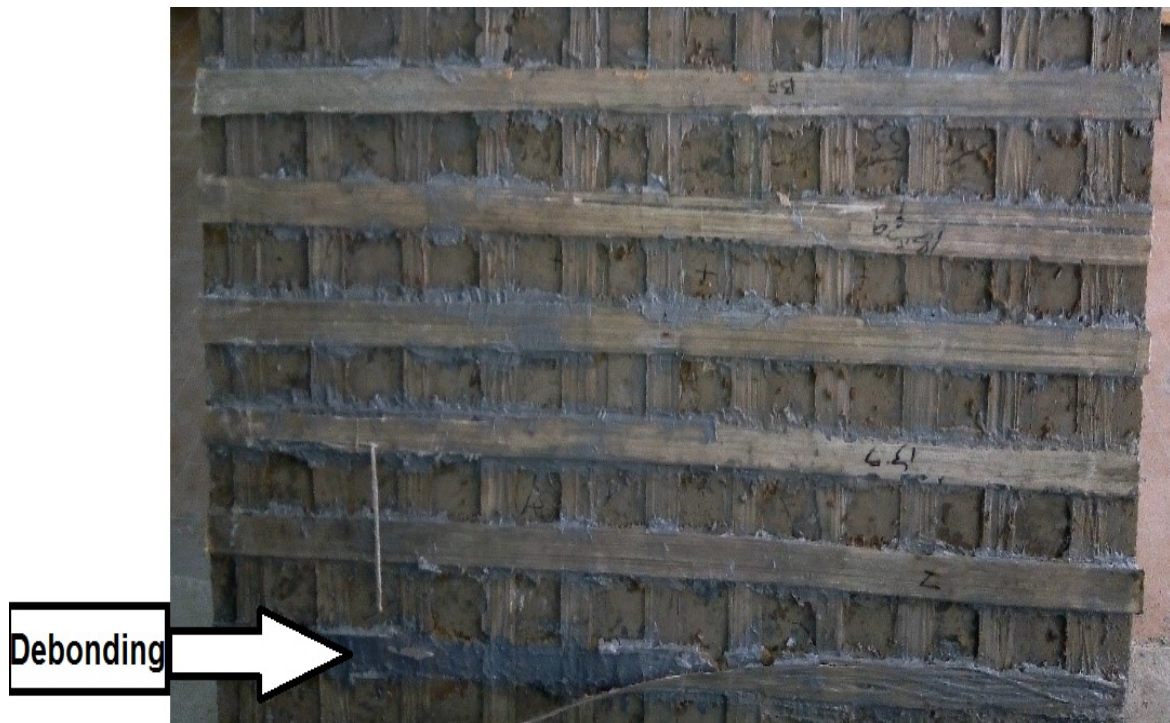364 **Fig. 19. Cracking pattern of specimen (G-3-10-Ag/2).**
365
366
367
368

369

370
371
372   **Fig. 20. Deponding shape for specimen (GS-1.5-20-Ag).**

373
374   **6. FINITE ELEMENT ANALYSIS**

375
376   In this part, the tested specimens were simulated using the FEA program ANSYS (version
377   15). The numerical results of the simulated slabs were compared with the experimental
378   results.

379   All the simulated models are simply-supported two way slabs subjected to four point load.
380   The concrete and resin are modeled with a higher order 3-D element named SOLID65.
381   LINK180 is used to define reinforcement steel and FRP bars while SOLID185 is used to
382   define FRP sheets.

383   Many materials were used in modeling the specimens such as concrete, steel reinforcement,
384   CFRP bars, GFRP bars, GFRP sheets and epoxy resin Sikadur® 330. The compressive
385   stress-strain relationship of concrete is considered to be linear from zero to one-half the
386   ultimate compressive strength, and the strain at the ultimate compressive strength ranges
387   from 0.002 to 0.003. Reinforcement bars and shear connectors were modeled as a nonlinear
388   and isotropic material. CFRP bars, GFRP bars and epoxy sikadur® 330 were modeled as
389   linear isotropic material. GFRP strips were modeled by linear orthotropic material. Table. 6
390   presents the properties of the used material

391

392

393

394
395 **Table. 6. The properties of the used materials.**
396

Material	Compressive strength (MPa)	Tensile strength (MPa)	Poisson`s ratio	Modulas of elasticity (GPa)
Concrete	25	2.8	0.2	20
Steel bars	--	340	0.3	200
GFRP bars	--	1370	0.3	76
CFRP bars	--	1400	0.3	210
GFRP strips	--	2250	0.3	76

397 The experimental results obtained from testing of the tested specimens are compared with
398 those obtained from the finite element modeling. The experimental and numerical results of
399 load versus mid-span deflection are compared for each specimen, as shown in Figs. (21 to
400 31). The typical deformed shape of the finite element models obtained by ANSYS (version
401 15) is as shown in Fig. 32. Table. 7 presents a comparison between the numerical and
402 experimental ultimate loads. It can be noticed that the ratio of the numerical ultimate load to
403 experimental one ranged from 0.95 to 1.12. It can be observed that ANSYS almost predicts a
404 higher ultimate load compared to the load observed during experiments.

405
406 **Table. 7. Comparison of experimental and numerical results.**
407

Specimen code	$P_{u, exp.}$	$P_{u, num.}$	$\dfrac{P_{u, num.}}{P_{u, exp.}}$
C	6.88	6.56	0.95
S-3-20-As	9.46	10.40	1.10
C-3-10-Ac/2	13.40	13.91	1.04
C-3-20-Ac	11.58	12.20	1.05
G-3-10-Ag/2	10.50	10.50	1.00
G-3-20-Ag	9.40	10.50	1.12
G-5-10-Ag/2	11.64	12.31	1.06
G-5-20-Ag	11.23	12.31	1.10
G-3-10-Ag	12.10	11.87	0.98
G-5-10-Ag	14.59	15.31	1.05
GS-1.5-20-Ag	11.74	11.60	0.99

408
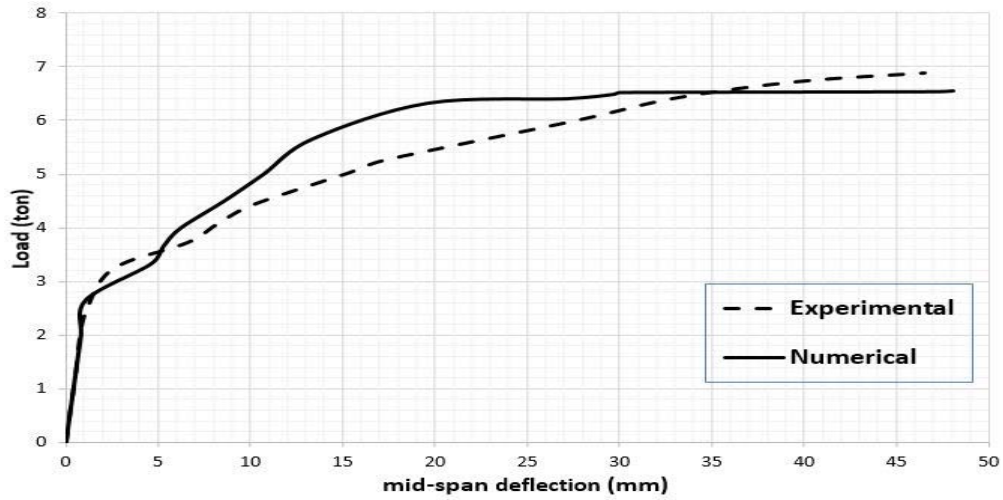
409
410
411 **Fig. 21. Comparison between experimental & numerical load-deflection curves of**
412 **tested specimen (C).**
413
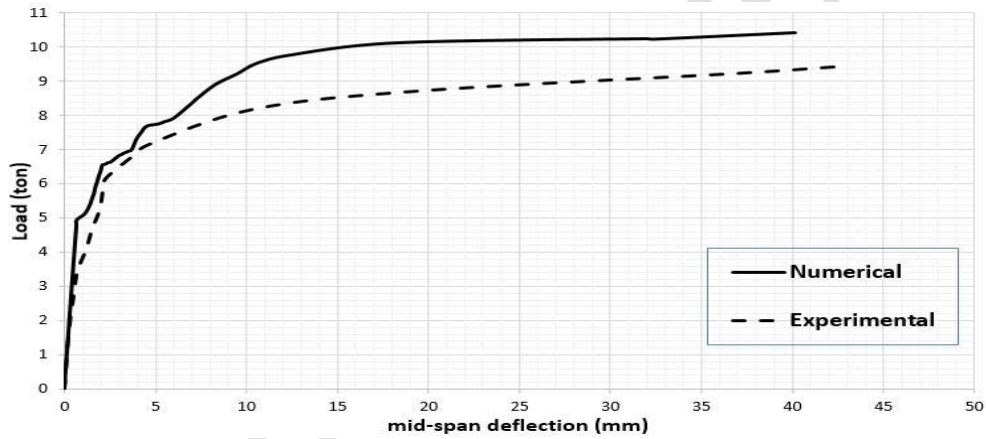
414
415
416 **Fig. 22. Comparison between experimental & numerical load-deflection curves of**
417 **tested specimen (S-3-20-As).**
418
419
420
421
422
423
424
425
426
427
428
429
430
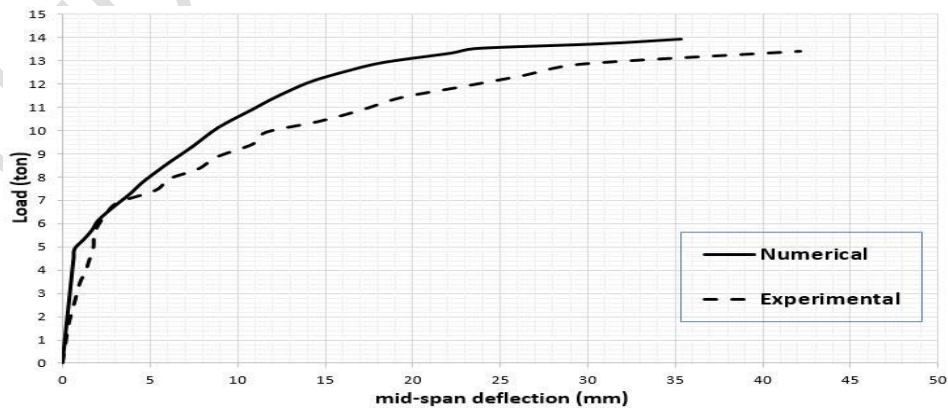
431
432 **Fig. 23. Comparison between experimental & numerical load-deflection curves of**
433 **tested specimen (C-3-10-Ac/2).**

434
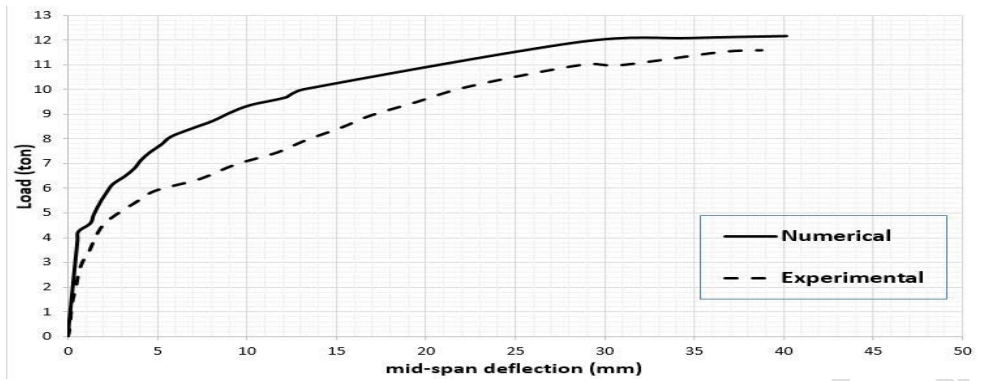
435
436 **Fig. 24. Comparison between experimental & numerical load-deflection curves of**
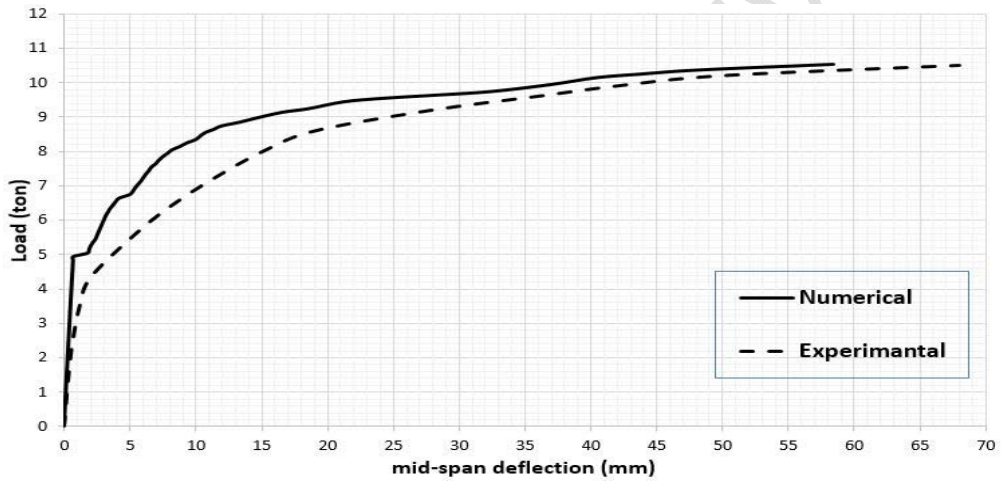437 **tested specimen (C-3-20-Ac).**
438

439
440
441 **Fig. 25. Comparison between experimental & numerical load-deflection curves of**
442 **tested specimen   (G-3-10-Ag/2).**
443
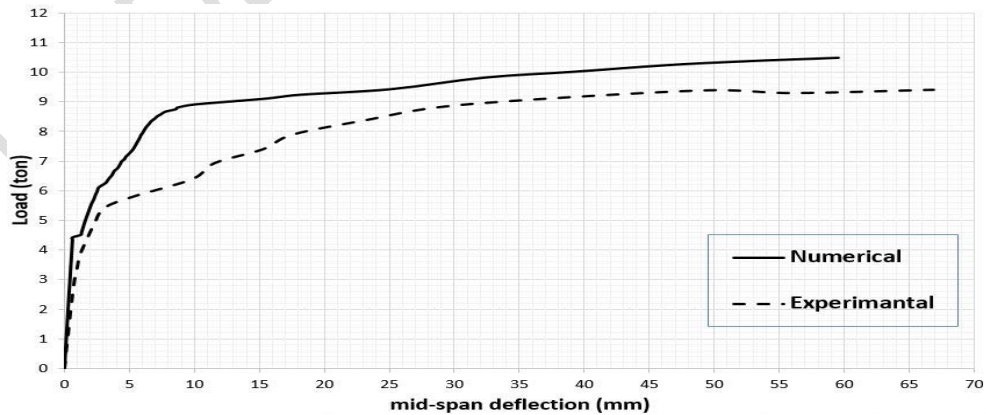
444
445 **Fig. 26. Comparison between experimental & numerical load-deflection curves of**
446 **tested specimen (G-3-20-Ag).**
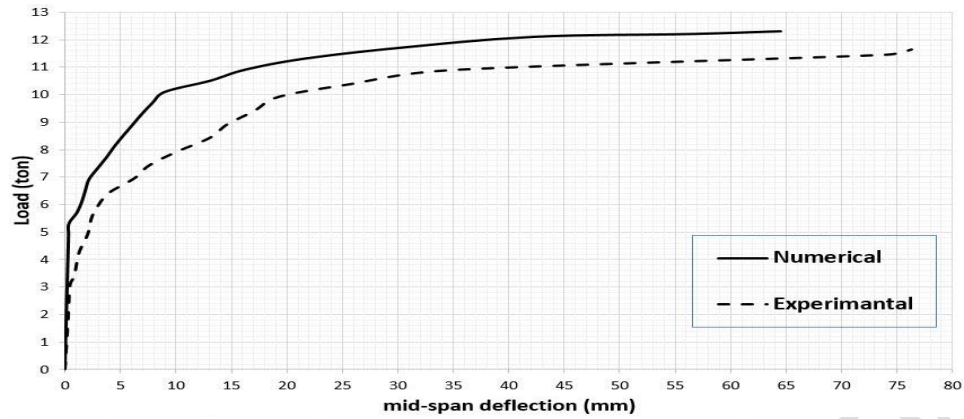
447
448
449   **Fig. 27. Comparison between experimental & numerical load-deflection curves of**
450   **tested specimen (G-5-10-Ag/2).**
451
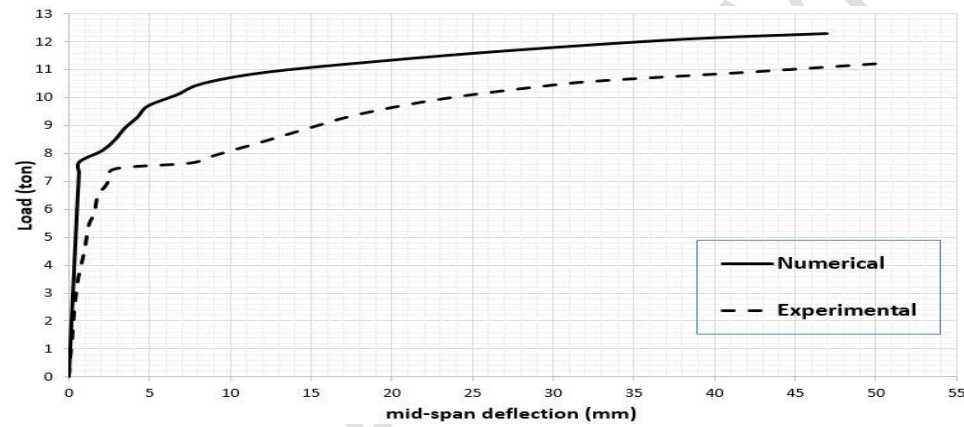
452
453
454   **Fig. 28. Comparison between experimental & numerical load-deflection curves of**
455   **tested specimen (G-5-20-Ag).**
456
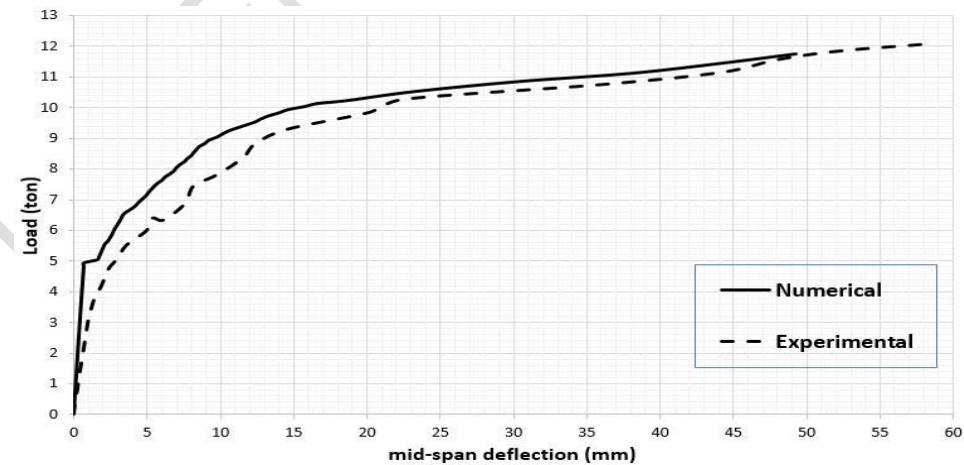
457
458
459   **Fig. 29. Comparison between experimental & numerical load-deflection curves of**
460   **tested specimen (G-3-10-Ag).**
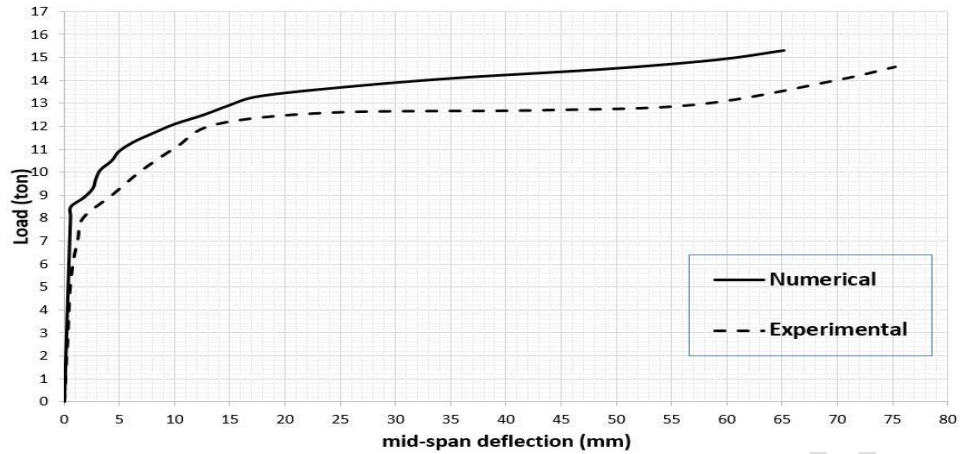
461
462
463   **Fig. 30. Comparison between experimental & numerical load-deflection curves of**
464   **tested specimen (G-5-10-Ag).**
465
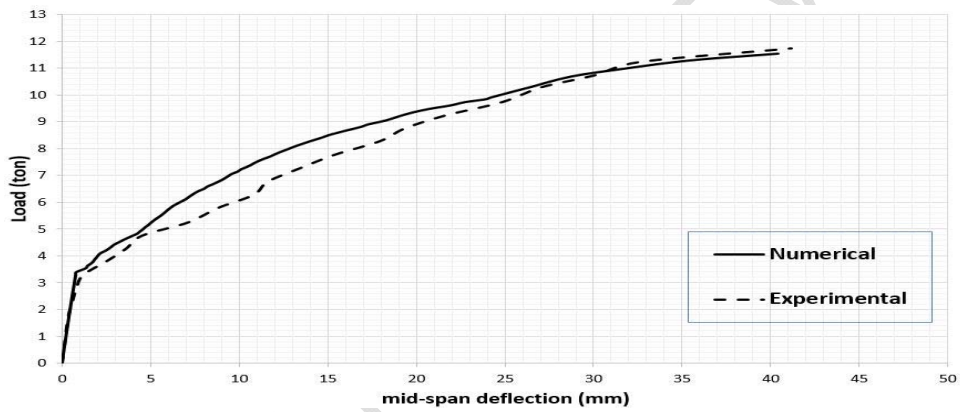
466
467
468   **Fig. 31. Comparison between experimental & numerical load-deflection curves of**
469   **tested specimen (GS-1.5-20-Ag).**
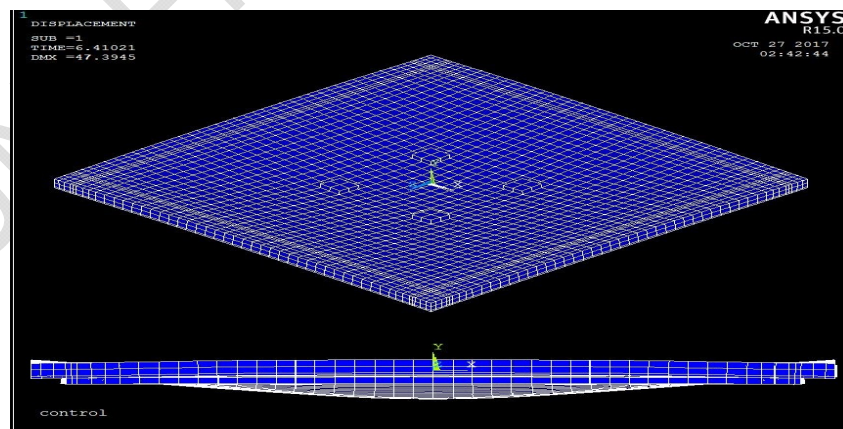470

471
472
473   **Fig. 32. Typical deformed shape of finite element model.**
474

7. CONCLUSIONS

The main goal of the current research is examining the effect of adding R.C layer reinforced by FRP elements on the structural behavior of two-way R.C slabs in terms of strength and flexure. From the experimental and numerical results, the following conclusions could be drawn as below:-

- Strengthening systems were effective in improving the flexural strength of the tested specimens by a range from 37% to 112%, also, the deflections were reduced significally by a range from 75.3% to 97.5% compared to the control specimen at its ultimate load.

- All methods used for strengthening of slabs in this research were effective to restore and improve the structural performance in terms of flexural rigidity, ultimate stiffness (Ku), initial cracking load and the ultimate carrying capacity.

- All the used materials in this research led to increase the initial cracking load by 50% to 300% and the ultimate load capacity also increased by 37% to 112%.

- For the three types of strengthening material (reinforcement steel, carbon fiber and glass fiber); the specimens (S-3-20-As, C-3-20-Ac & G-3-20-Ag) achieved an increase in the initial cracking load by 100%, for the three specimens, and the ultimate capacity by 38%, 68% and 37%, respectively.

- For the strengthening layer thickness (30 & 50 mm); the specimens (G-3-10-Ag/2 & G-5-10-Ag/2) achieved an increase in the initial cracking load by 125% and 155%, respectively, and the ultimate capacity by 53% and 69%, respectively, also, the specimens (G-3-20-Ag & G-5-20-Ag) achieved an increase in the initial cracking load by 100% and 100%, respectively, and the ultimate capacity by 37% and 63%, respectively, also, the specimens (G-3-10-Ag & G-5-10-Ag) achieved an increase in the initial cracking load by 50% and 300%, respectively, and the ultimate capacity by 76% and 112%, respectively.

- For the spacing between reinforcement bars (100 & 200 mm); the specimens (G-3-10-Ag/2 & G-3-20-Ag) achieved an increase in the initial cracking load by 125% and 100%, respectively, and the ultimate capacity by 53% and 37%, respectively, also, the specimens (G-5-10-Ag/2 & G-5-20-Ag) achieved an increase in the initial cracking load by 155% and 100%, respectively, and the ultimate capacity by 69% and 63%, respectively, also, the specimens (C-3-10-Ac/2 & C-3-20-Ac) achieved an increase in the initial cracking load by 150% and 100%, respectively, and the ultimate capacity by 95% and 68%, respectively.

- For the reinforcement bars area (A & 2A); the specimens (G-3-10-Ag/2 & G-3-10-Ag) achieved an increase in the initial cracking load by 125% and 50%, respectively, and the ultimate capacity by 53% and 76%, respectively, also, the specimens (G-5-10-Ag/2 & G-5-10-Ag) achieved an increase in the initial cracking load by 155% and 300%, respectively, and the ultimate capacity by 69% and 112%, respectively.

- For the strengthening method (FRP bars & FRP strips); the specimens (G-3-20-Ag & GS-1.5-20-Ag) achieved an increase in the initial cracking load by 100% and 175%, respectively, and the ultimate capacity by 37% and 71%, respectively.

- For all the tested specimens, it was observed that the failure was flexural failure due to partial debonding between the strengthening layer and the original slab also, it was observed that the cracks began firstly at the slab tension side under four point load forming square line and with increasing the load, number and width of the cracks increase and begin to propagate in diagonal direction towards the slab edge.

- In general, the specimen (G-5-10-Ag) was the best one, which led to the highest ultimate capacity between the tested specimens. However the CFRP bars was the best material, which led to the highest improvement in the rigidity and ultimate capacity of the tested specimens.

- The numerical results used to predict the ultimate capacity of the tested specimens gave moderate conservative values, where the ratio of the numerical ultimate load and experimental one ranged between 0.95 to 1.12.

Authors' contributions

This work was carried out in collaboration between all authors. All authors read and approved the final manuscript.

REFERENCES

[1] Heiza K, Nabil A, Maleka N and Tayel M. (2014). State of the art review: Strengthening of reinforced concrete structures-different strengthening techniques. 16th international conference on nano technology in construction, Cairo, Egypt, March.

[2] Fernandes H, Lucio V and Ramos A (2017). Strengthening of RC slabs with reinforced concrete overlay on tensile face. Engineering structure.137, 540-550.

[3] Al-kubaisy, MA and Jumaat MZ (2000). Flexural behavior of reinforced concrete slabs with ferrocement tensions cover. J.Constr.Build. Mater., 14, 245-252.

[4] Ezzat, H F, Yousry BI, and Yasser SK (1996). Repairing reinforced concrete slabs using ferrocement laminates. 7th international colloquium on structural and geotechnical engineering, Cairo, Egypt, December.

551   [5] Calixto JM, Pires E F, Lima SA and Piancastelli EM (2003). Behavior of reinforced
552   concrete slabs strengthened in flexure by concrete overlays. ACI Structural Journal 229,
553   p.389-406.
554
555   [6] Michel L, Ferrier E, Agbossou A and Hamelin P (2009). Flexural stiffness modelling of
556   R.C slab strengthened by externally bonded FRP. Composites: part B 40, p.758-765.
557
558   [7] Foret G and Limam O (2008). Experimental and numerical analysis of RC two-way slabs
559   strengthened with NSM CFRP rods. J.Constr.Build. Mater., 22, 2025-2030.
560
561   [8] Foret, G, Limam O and Ehrlacher A (2003). RC two-way slabs strengthened with CFRP
562   strips: experimental study and limit analysis approach. Composite structure. 60, 467-471.
563
564   [9] Tan KY, Tumialan G and Nanni A (2003). Evaluation of externally bonded CFRP system
565   for the strengthening of RC slabs. Department of civil engineering, university of Missouri,
566   Rolla, USA.
567
568   [10] Al-Rousan R, Issa M and Shabila H (2012). Performance of reinforced concrete slabs
569   strengthened with different types and configuration of CFRP. Composites: part B 43, p.510-
570   521.